NBSIR 76-1164 (R) CE38009
Div 31303

~~FE-1749-9~~
Dist. Category UC-90C

MATERIALS RESEARCH FOR CLEAN UTILIZATION OF COAL

QUARTERLY PROGRESS REPORT
October 1976

Samuel J. Schneider
Project Manager

Institute for Materials Research
National Bureau of Standards
Washington, D. C. 20234

PREPARED FOR THE UNITED STATES
ENERGY RESEARCH AND DEVELOPMENT ADMINISTRATION

Under Contract No. 14-32-0001-1749

"This report was prepared as an account of work sponsored by the United States Government. Neither the United States nor the United States ERDA, nor any of their employees, nor any of their contractors, subcontractor, or their employees, makes any warranty, express or implied, or assumes any legal liability or responsibility for the accuracy, completeness, or usefulness of any information, apparatus, product or process disclosed, or represents that its use would not infringe privately owned rights."

Schneider, S. J., Materials research for clean utilization of coal. Quarterly progress report October 1976, Energy Research and Development Administration FE-3800-9, 32 pages (Available from the National Technical Information Services, Springfield, VA 1976).

313

NBSIR 76-1164

1715a

TABLE OF CONTENTS

PAGE

I. OBJECTIVE AND SCOPE OF WORK. 1

II. SUMMARY OF PROGRESS TO DATE. 1

III. DETAILED DESCRIPTION OF TECHNICAL PROGRESS 2

1. Metal Corrosion. 2

a. Constant Strain-Rate Test. 2

b. Pre-Cracked Fracture Test. 13

c. Erosive Wear 13

2. Ceramic Deformation, Fracture and Erosion. 20

3. Chemical Degradation 24

a. Reactions and Transformations. 24

b. Slag Characterization. 25

c. Vaporization and Chemical Transport. 25

4. Failure Prevention 26

I. OBJECTIVE AND SCOPE OF WORK

Coal Gasification processes require the handling and containment of corrosive gases and liquids at high temperature and pressures, and also the handling of flowing coal particles in this environment. These severe environments cause materials failures which inhibit successful and long-time operation of the gasification systems. This project entails investigations on the wear, corrosion, chemical degradation, fracture, and deformation processes which lead to the breakdown of metals and ceramics currently being utilized in pilot plants. Studies will also be carried out on new candidate materials considered for improved performance. Special emphasis will be devoted to the development of test methods, especially short-time procedures, to evaluate the durability of materials in the gasification environments. These methods will focus on wear, impact erosion, stress corrosion, strength, deformation, slow crack growth and chemical degradation of refractories. A system has been initiated to abstract and compile all significant operating incidents from coal conversion plants. This program will provide a central information center where problems of common interest can be identified and analyzed to avoid unnecessary failures and lead to the selection of improved materials for coal conversion and utilization. Active consultation to ERDA and associated contractors will be provided as requested.

II. SUMMARY OF PROGRESS TO DATE

The summary of progress is contained in the individual task progress and plans - Section III.

III. DETAILED DESCRIPTION OF TECHNICAL PROGRESS

1. Metal Corrosion

a. Constant Strain-Rate Test (G.M. Ugiansky and C.E. Johnson, 312.04)

Progress: To further elucidate the relationship between sensitization of 310 stainless steel (SS) and the susceptibility to intergranular embrittlement at elevated temperatures, tests were carried out on 310 S stainless steel (a low carbon 310 SS which is designed to resist sensitization). The 310 S stainless steel was tested at 1000°F at a strain rate of $1 \cdot 10^{-6}$ s^{-1} in a vacuum (726 mm Hg). The reduced section of the specimen still showed some cracking, but the elongation and reduction in area were twice as great as for the 310 SS. Some necking could be detected. This was evidence that the lower carbon content in the alloy lowers the susceptibility to intergranular embrittlement but does not prevent it. The use of 310 S stainless steel in place of Type 310 SS also slows the rate of sensitization but does not prevent it (1). Type 347 stainless steel (similar to 304 SS but stabilized with niobium and tantalum) was tested at 1000°F at a strain rate of $1 \cdot 10^{-6}$ s^{-1}. The resultant fractures were ductile with a large reduction in area (66%), but the elongation was low (16%). No cracking was apparent in the reduced section of the specimens. The tests of this alloy showed that intergranular embrittlement can be prevented by using stabilized alloys. These tests also further illustrate that reduction in area is probably a better indicator than elongation for measuring susceptibility to stress corrosion cracking (SCC), especially when comparing different alloys. Fig. 1 shows the fractures of 347, 310 S, and 310 SS when tested at 1000°F in a vacuum (726 mm Hg) at a strain rate of $8.4 \cdot 10^{-7}$ s^{-1}.

Type 310 SS was also tested at temperatures of 1500°F and 1900°F. These temperatures were chosen to look at the effect of sensitization on intergranular embrittlement as a function of test temperature. The sensitization temperature range is 800-1650°F. With tests already completed at 1000°F (in the middle of the sensitization range), the 1500°F tests would give information near the top of the range, and the 1900°F tests would give results for testing well above the sensitization range. These tests were run at a constant strain rate of $1 \cdot 10^{-6}$ s^{-1} in air because the present test chambers were not designed for these high temperatures. At 1500°F, the ultimate tensile strength was only 25 KSI versus 60 KSI when tested at 1000°F. The elongation was 11% which is a lower value than any obtained for tests on 310 SS at 1000°F. The reduction in area was 14.5%, which is a lower value than any obtained for that parameter for any tests on 310 SS at 1000°F.

The 1900°F test still resulted in a fracture that seemed to be brittle. The reduction in area was only 21% which compares to 18% for 310 SS

when tested at 1000°F. The elongation was 41% which was probably due to the high ductility of the non-embrittled portions of the specimen. The ultimate tensile strength was only 11 KSI when tested at the slow strain rate of $1 \cdot 10^{-6}$ s^{-1}.

The series of tests that were requested by Dr. T.B. Cox, the project monitor, to be run on 310, 310 S, 347 SS, and Incoloy 800 in wet H_2S at 1000°F over a range of strain rates have been completed except for one specimen of each alloy at the very slow strain rate of $1 \cdot 10^{-7}$ s^{-1}.

The resulting parameters measured for 310 stainless steel when tested in wet H_2S at 1000°F are tabulated in Table 1.

Table 1. Properties of 310 stainless steel tested in wet H_2S[1] and H_2O/H_2S[2] at 1000°F.

Strain Rate, s^{-1}	Gas	UTS, KSI	Elongation, %	Reduction in Area, %
$1.3 \cdot 10^{-4}$	2	82	33.8	63.2
$7.8 \cdot 10^{-5}$	1	73	32.9	55.9
$5.5 \cdot 10^{-5}$	2	76	33.4	62.8
$7.2 \cdot 10^{-6}$	2	68.5	22.5	33.1
$3.9 \cdot 10^{-6}$	1	70	22.9	25.4
$3.6 \cdot 10^{-6}$	2	69	23.7	30.2
$1.1 \cdot 10^{-6}$	1	68	17.2	18.4
$8.4 \cdot 10^{-7}$	2	68	18.7	17.5

[1] Wet H_2S = H_2S saturated with water vapor at room temperature.

[2] H_2O/H_2S = H_2S plus steam.

The plot of percent reduction in area versus strain rate for 310 SS (Fig. 2) shows that as the strain rate decreases, the reduction in area decreases from 63% to 17%. The difference between the environments of wet H_2O/H_2S is that the wet H_2S signifies the water vapor saturated H_2S at room temperature, whereas, the H_2O/H_2S is a steam and H_2S gas mixture. These two corrosive environments do not seem to have any effect on the lowering of the properties of 310 SS since the equivalent reduction in properties can be obtained when the specimens are tested in helium, argon, or vacuum.* When the

*None of the environments used was O_2 or H_2O free as seen by the oxide films of various thicknesses that was always present after testing.

request was made to test these different alloys over a range of strain rates at 1000°F, the decision to use the wet H_2S environment was made.

The 310 S stainless steel (lower in carbon content, 0.25% max. for 310 compared to 0.08% max. for 310 S) was tested in wet H_2S at 1000°F and was found to behave quite differently than 310 when tested over the same range of strain rates. The measured properties are tabulated in Table 2.

Table 2. Properties of 310 S stainless steel tested in wet H_2S at 1000°F

Strain Rate, s^{-1}	UTS, KSI	Elongation, %	Reduction in Area, %
$1.3 \cdot 10^{-4}$	71.5	33.6	63.0
$3.7 \cdot 10^{-5}$	71.6	34.5	62.6
$7.3 \cdot 10^{-6}$	69.0	35.9	62.3
$8.4 \cdot 10^{-7}$	63.1	34.8	50.1

The plot of percent reduction in area versus strain rate (Fig. 3) shows that the reduction in area remains constant at around 63% until the slow strain rate of approximately $1 \cdot 10^{-6}$ s^{-1} is reached when the reduction in area begins to decrease somewhat. A test at the very slow strain rate of $1 \cdot 10^{-7}$ s^{-1} should indicate whether the decrease is significant and if the percent reduction in area decreases to a value comparable to that obtained with 310 stainless steel. This curve shows how the low carbon content in 310 S retards the process of intergranular embrittlement but does not prevent it after a long period of time at temperature, as is also the case for sensitization (1).

The measured properties of the stabilized 347 stainless steel that were tested in wet H_2S over a range of strain rates at 1000°F are tabulated in Table 3.

Table 3. Properties of 347 stainless steel tested in wet H_2S at 1000°F

Strain, Rate, s^{-1}	UTS, KSI	Elongation, %	Reduction in Area, %
$1.3 \cdot 10^{-4}$	78.8	17.4	62.0
$3.7 \cdot 10^{-5}$	78.1	15.5	63.1
$7.3 \cdot 10^{-6}$	71.6	15.1	64.3
$8.4 \cdot 10^{-7}$	75.6	14.5	55.4
$8.4 \cdot 10^{-7}$	75.4	17.1	61.4

The curve of percent reduction in area versus strain rate (Fig. 4) shows that the percent reduction in area remains constant for 347 SS over the range of strain rates tested.

The results of Incoloy 800 tested in wet H_2S over a range of strain rates are tabulated in Table 4.

Table 4. Properties of Incoloy 800 tested in wet H_2S at 1000°F

Strain Rate, s^{-1}	UTS, KSI	Elongation, %	Reduction in Area, %
$1.3 \cdot 10^{-4}$	--	32.8	68.8
$3.7 \cdot 10^{-5}$	--	33.5	65.3
$7.3 \cdot 10^{-6}$	--	34.2	55.2
$8.4 \cdot 10^{-7}$	--	32.0	49.9

The curve in Fig. 5 shows the decrease of reduction in area from 69% to 50% as the strain rate decreases from 10^{-4} to approximately 10^{-6} s^{-1} for the Incoloy 800.

In order to change the testing apparatus to be able to handle the gas mixtures being used at Battelle Labs. and Argonne National Lab., some design work had to be done. Contacts with Wright and Peterson of Battelle and Nateson of Argonne were made to discuss their methods of getting water into their systems. We made the decision to use steam and ordered a small steam generator.

Commercial gas suppliers were contacted to determine the availability of gas mixtures. Mixtures of CO, CO_2, and H_2 in specific proportions can be obtained but not with H_2S or water.

Several problems arose during the quarter. A failure of a printed circuit board in the data gathering facility delayed the starts of the 310 S, 347, and In 800 tests. A sensing element failure in the data gathering facility resulted in loss of UTS data for all In 800 tests. A DC-differential transformer failed on one of the test machines, thus preventing strain measurements on that specimen during the test run. The Inconel 671 rod was received, but none of the material was suitable for machining the needed 23 inch long specimens. The material was sent back to the supplier to be straightened.

Plans: Types 310, 310 S, 347 stainless steel, and Incoloy 800 will be tested at the very slow strain rate of $1 \cdot 10^{-7}$ s^{-1} in wet H_2S at 1000°F. Inconel 671 will be tested over the range of strain rates at 1000°F in wet H_2S after the alloy rods have been straightened. During the time before the gas mixing apparatus is completed and installed, the possible mechanisms of intergranular embrittlement of 310 SS will be investigated.

The mechanism of failure of the 310 SS will be investigated by testing this steel in vacuum or a reducing atmosphere with more precautions taken to remove all oxygen and water. These tests will be run to determine whether or not the susceptibility of 310 SS is actually environment insensitive. Since an oxide film was always present and the cracks seem to initiate at the surface, it is believed that the embrittlement may be due to oxidation of the chromium depleted grain boundary region or possibly due to hydrogen attack.

References

1. Heat Treating of Stainless Steels, Source Book on Stainless Steels — ASM Engineering Bookshelf (1976), p. 163.

Fig. 1. Fractures of 347, 310S, and 310 stainless steels from left to right, respectively. Tests conducted in vacuum (726 mm Hg) at 1000°F at a strain rate of $8.4 \cdot 10^{-7}$ s^{-1}. 2.5x

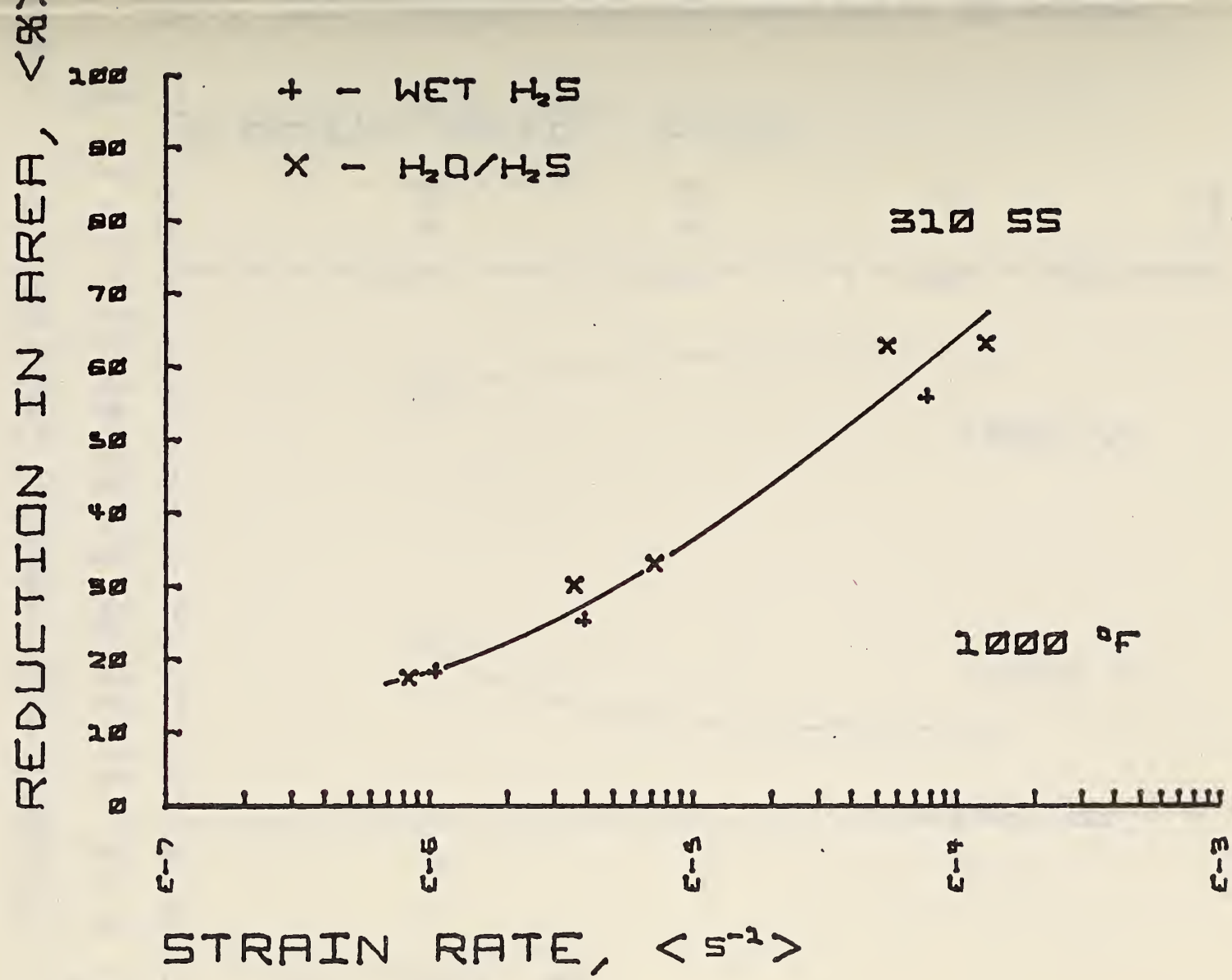

Fig. 2. Curve of reduction in area versus strain rate for 310 stainless steel. Tests conducted in saturated H_2S (wet H_2S) and in steam and H_2S (H_2O/H_2S) at 1000°F.

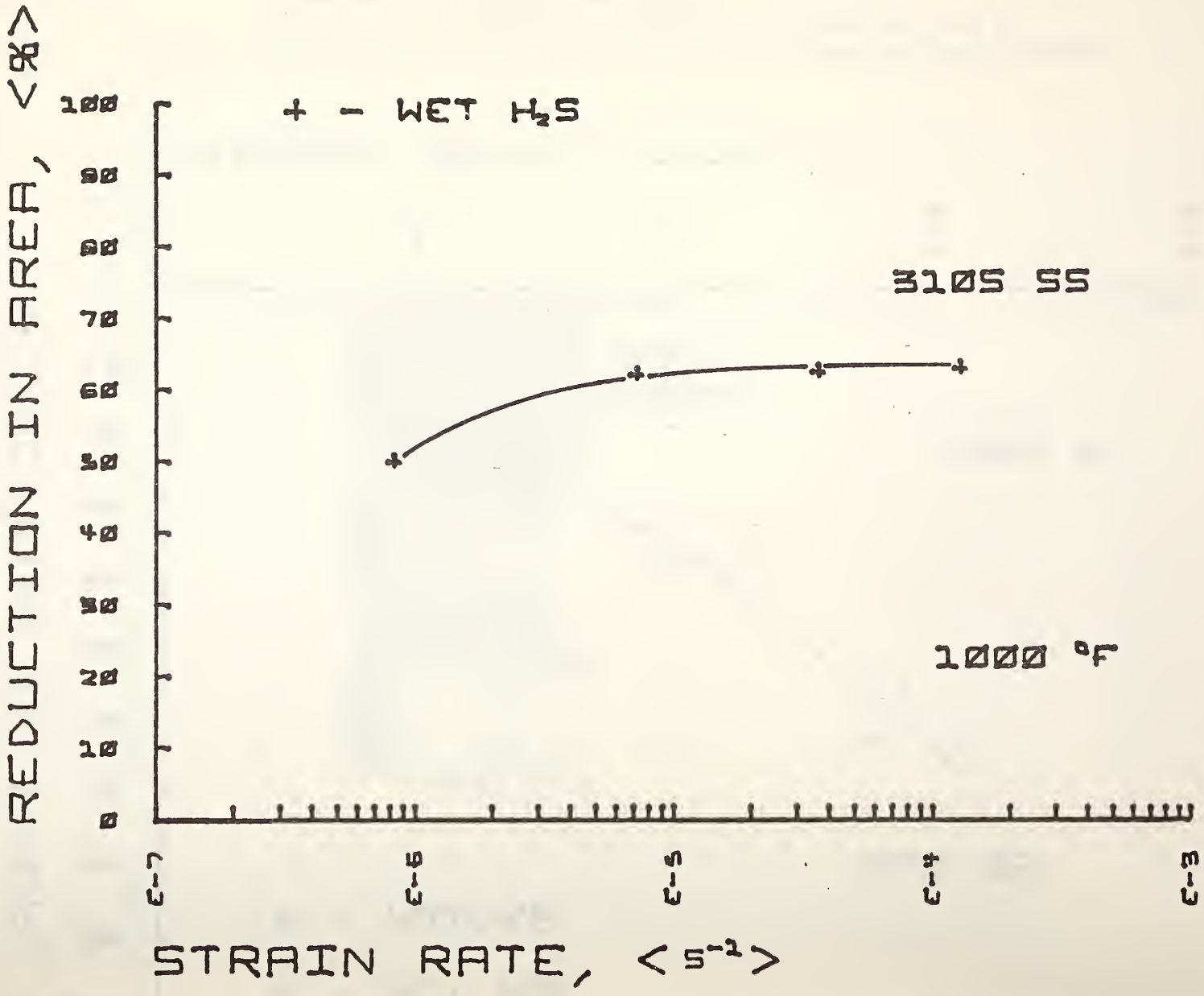

Fig. 3. Curve of reduction in area versus strain rate for 310S stainless steel. Tests conducted in saturated H_2S (wet H_2S) at 1000°F.

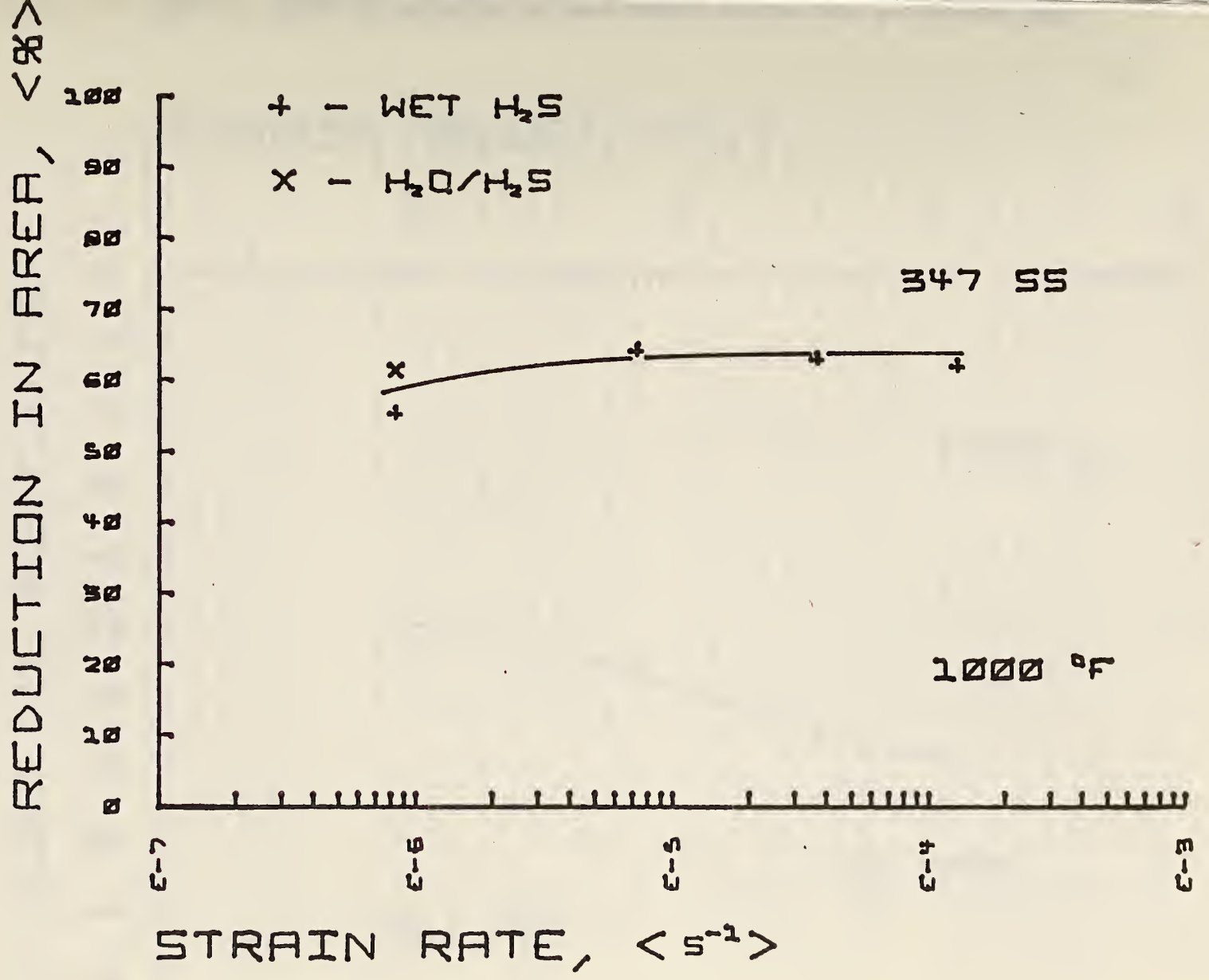

Fig. 4. Curve of reduction in area versus strain rate for 347 stainless steel. Tests conducted in saturated H_2S (wet H_2S) and in steam and H_2S (H_2O/H_2S) at 1000°F.

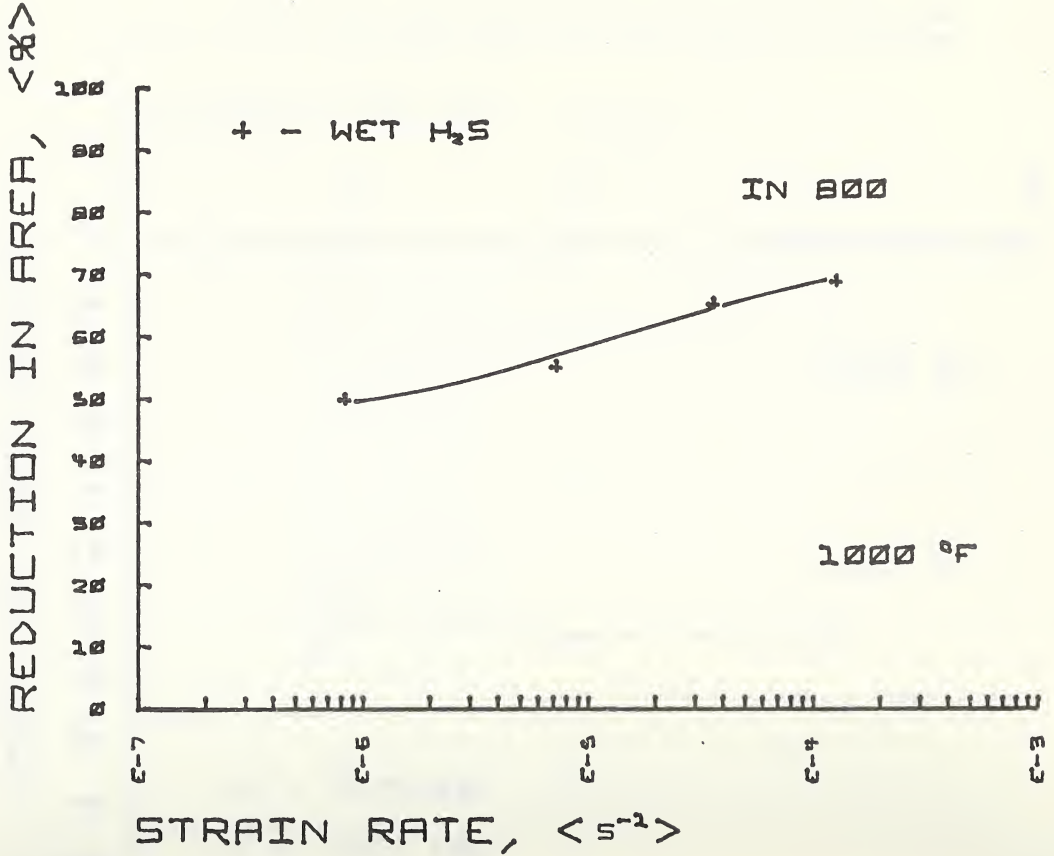

Fig. 5. Curve of reduction in area versus strain rate for Incoloy 800. Tests conducted in saturated H_2S (wet H_2S) at 1000°F.

b. Pre-Cracked Fracture Test (J. H. Smith, 312.01)

Work is not scheduled to begin until 1977.

c. Erosive Wear (A. W. Ruff, L. K. Ives, J. Young, 312.03)

Progress: Tests were conducted in the flame-erosion apparatus to determine the angular dependence of erosion of 310 stainless steel at 25°C and 975°C. As in previous work, SiC abrasive particles of 100 mesh size were employed as the eroding media. Particles were supplied at a rate to yield a flux of approximately 0.04 g/cm^2s. In some tests, a flux as high as 0.08 g/cm^2s was used, however, this did not produce an appreciable change in relative erosion rate. Tests at 25°C were conducted in air while those at 975°C were carried out in a combustion gas atmosphere produced by burning an air, oxygen and propane mixture. An excess amount of oxygen above that needed for complete combustion of the propane was supplied to yield a relatively strongly oxidizing atmosphere. An analysis of the gas composition under the specific conditions of these tests was not obtained. However, based on previous results under similar conditions, a composition of about 65% N_2, 10%O_2, 10%CO_2 and 15% H_2O would be expected. The particle velocity at both 25°C and 975°C was maintained at approximately 34 m/s.

Figure 1 shows a sample with the protective metal shield that is used to prevent erosion of the otherwise exposed top edge. The sample is clamped in a ceramic holder specifically designed for elevated temperature tests but also used at 25°C. A cylindrical heat shield (not shown) was employed to reduce the temperature gradient along the exposed specimen face to about 20°C at 975°C. It was indicated in an earlier monthly report, as a result of some preliminary data, that this heat shield might disturb the flow of particles and thereby affect the erosion rate. A number of tests have now been conducted at 25°C with and without the heat shield in place. The results indicate that the erosion rate is not affected by the heat shield.

Results of angular dependence tests at 25°C and 975°C are plotted in Fig. 2. Each point in Fig. 2 represents the accumulated average of a number of tests of approximately one hour duration on a single sample. At 25°C, a rather broad maximum occurs at 15-30° followed by a minimum at 90° (particle stream normal to the surface). This behavior is typical of ductile materials in general. A substantial departure from this behavior is indicated at 975°C. The maximum now occurs at 90° while only an inflection is apparent at 20°-30°. This angular dependence might be attributed to the fact that a relatively thick oxide layer exists on the specimen surface at 975°C under oxidizing conditions. Studies described in the last quarterly report (April - June 1976) indicated that the impacting particles probably did not penetrate this layer at a velocity of 34 m/s. Thus, the eroding

material should be treated as an oxide rather than a metal. At sufficiently low temperatures, such oxide materials fail by a brittle fracture mechanism and exhibit a characteristically different angular dependence then ductile metals. Namely, a maximum in erosion rate occurs at 90° with a decreasing rate at lower angles. The shape of the curve in Fig. 2 obtained at 975°C suggests the superposition of ductile and brittle characteristics. However, it is difficult to rationalize a brittle oxide behavior at 975°C. Indeed, the topography of impact craters at 90° (April - July 1976 quarterly report) suggests a ductile mode of formation. Furthermore, the work of Wiederhorn et al. (See previous quarterly reports) on refractory materials has shown that, while these materials exhibit brittle erosion behavior at 25°C, their angular erosion dependence is that of a ductile material at 1000°C.

The nature of the corroded-eroded sample surfaces and the mechanisms by which erosion occurs is undoubtedly quite complex under the conditions of these tests. There is some indication that the erosion rate gradually decreased with exposure time at 975°C. Erosion loss is plotted against test number for different angles at 25°C in Fig. 3 and 975°C in Fig. 4. For a given angle, each test (approximately 1 hr.) represents exposure of the sample surface to the same quantity of abrasive. At 25°C, Fig. 3 suggests that the erosion rate was nearly constant with test number; possibly, a slight increase is indicated. In Fig. 4, continued exposure at 975°C appears to result in a decrease in erosion rate at all angles except 30°. It is thought that part of the protection shield was worn away in the latter case. At other angles, the decrease may be due to a gradual change in the nature of the exposed surface due to corrosion related effects. That is, a steady state or balanced condition between oxidation and erosion effects may not have been attained. It should be noted in these tests that both the particle flux and gas flow, in a direction normal to the specimen surface, decrease with decreasing angle of attack. Thus at 15°, the particle flux in a direction normal to the specimen surface is approximately one-quarter of that at 90°. Recognizing that the process under consideration is one of combined erosion and corrosion, the direct comparison of results plotted in Fig. 2 may not be valid. Additional tests at different particle velocities and fluxes should lead to clarification of this question.

Results of previous tests have shown that the abrasive flow rate in the Roberts Jet Abrader was not critical in determining the relative erosion rate (specimen wt. loss/wt. abrasive) of a particular specimen as long as the flow rate was known and could be maintained. A series of erosion tests were recently made at nozzle pressure drops of 1/4, 1/2 and 1 psig (which are proportional to the abrasive flow rate) to further determine the flow rate sensitivity. The data

shown below were obtained using different pressure reducing valves (PRV) on the gas supply tank. Specimens of 304 stainless steel and 50μm Al_2O_3 abrasive were used with the usual eroding conditions (40 psig propellent gas, nozzle at 45°, 1 cm distance, for 2 min.) and 5 runs in each condition.

PRV No.	Nozzle Pressure Drop (psig)	Av. Wt. Loss (mg)	Deviation (mg)
1	1/4	2.2	1.2
1	1/2	3.9	0.3
1	3/4	3.5	0.6
2	1/4	2.6	0.2
2	1/2	1.9	0.2
2	1	3.8	0.4
2	1/4	1.4	0.7
2	1/2	1.9	0.2

Investigation into the cause of the larger deviations in erosion values revealed that PRV#1 was not returning to the same pressure each time the eroder gas line valve was activated. This resulted in a changed nozzle pressure and an erroneous signal to the electronic flow controller on the system. This caused a greater change in abrasive flow than would otherwise occur with a slight change in propellent gas pressure. To correct this source of flow variation a second pressure transducer has been connected to the gas line ahead of the abrasive chamber. The circuit of the abrasive flow controller has been modified to integrate the signal from this second transducer, compensating for main line pressure changes and maintaining the abrasive flow more constant.

Specimens installed in the Morgantown Energy Research Center (MERC) experimental gasifier system in March 1976 (see January - March 1976 quarterly report) were retrieved on September 17, 1976. A preliminary examination of the specimens revealed that a significant erosion loss had occurred in at least one case. Additional effects resulting from the deposit of soot, tar and from corrosion were also observed. Changes that occurred in the specimens are currently being analyzed in detail. The data will be reported and an evaluation of the results given in a future report.

Plans: This task has been terminated as of the current reporting period, however, a report on the above activities will be provided when the data is available.

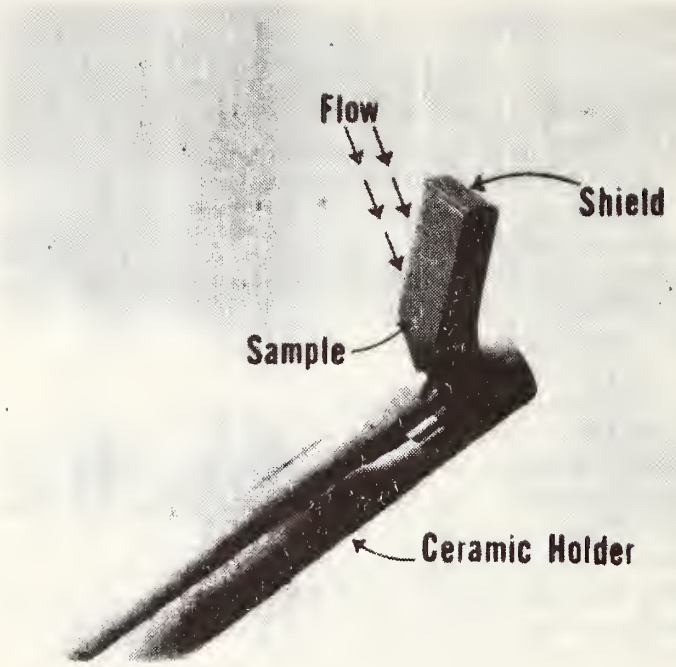

Fig. 1. 310 stainless steel erosion test specimen with protective shield in place.

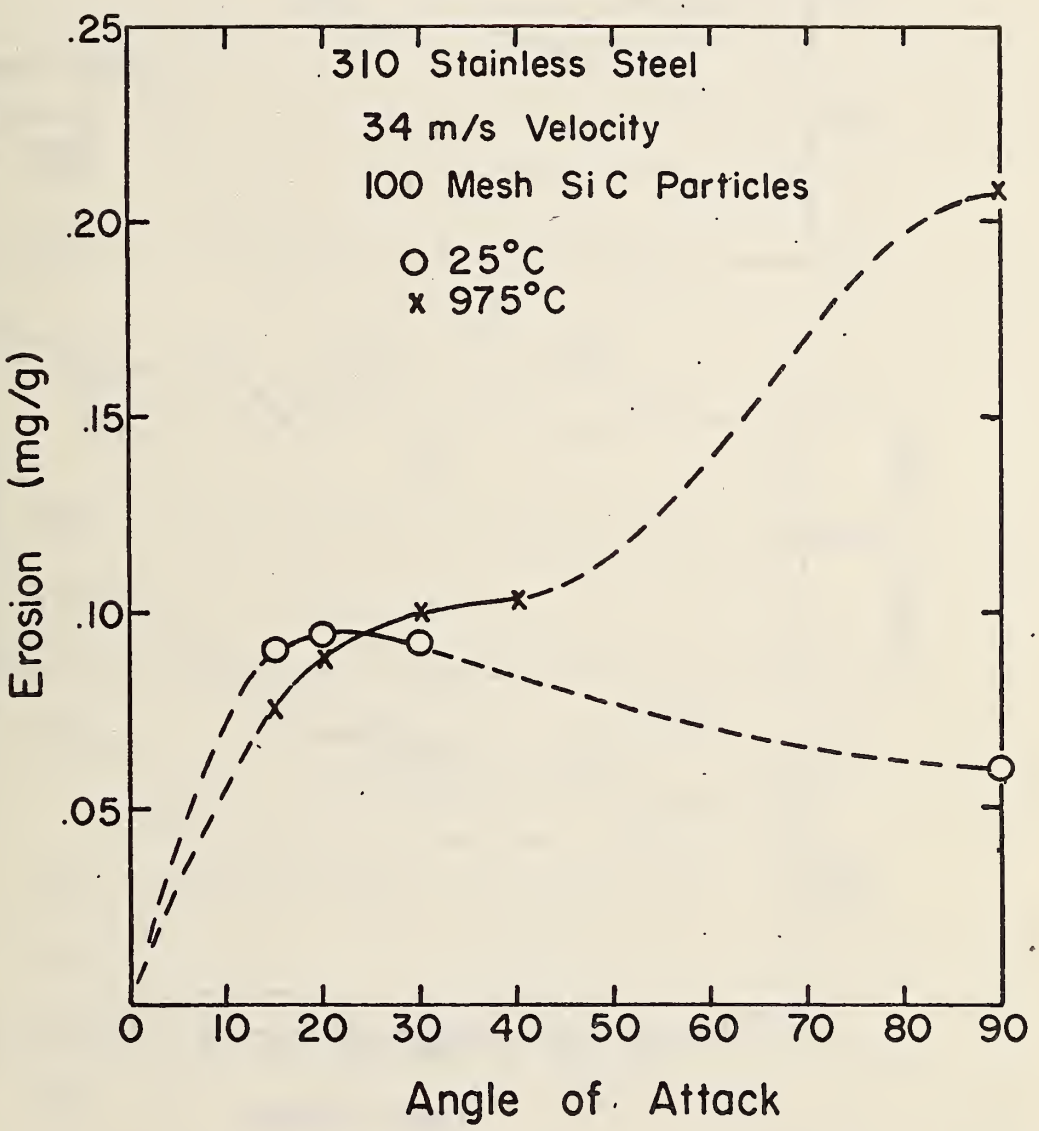

Fig. 2. Angular dependence results on erosion of 310 stainless steel at 25°C and 975°C.

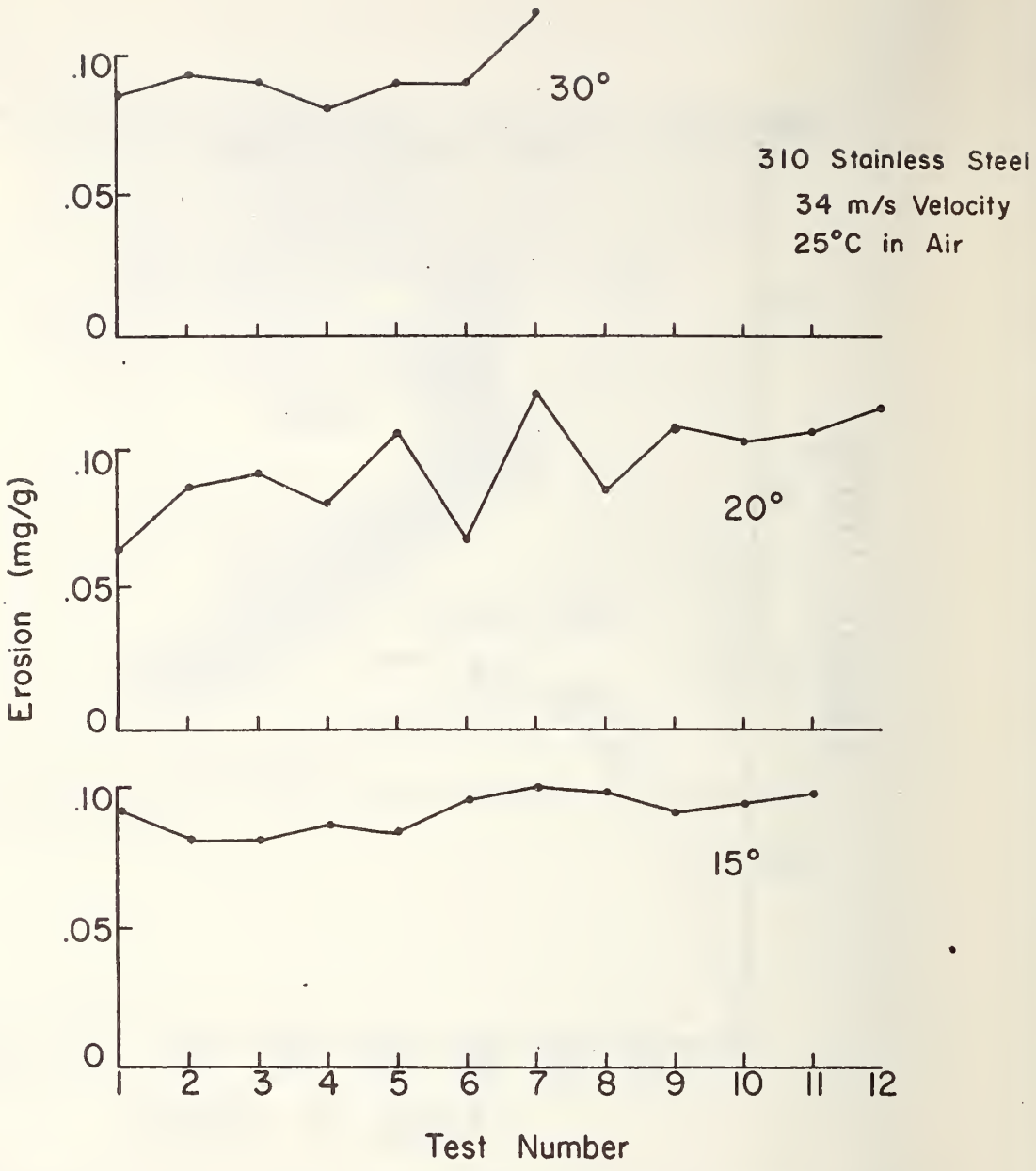

Fig. 3. Trend of erosion rate with test number at 25°C.

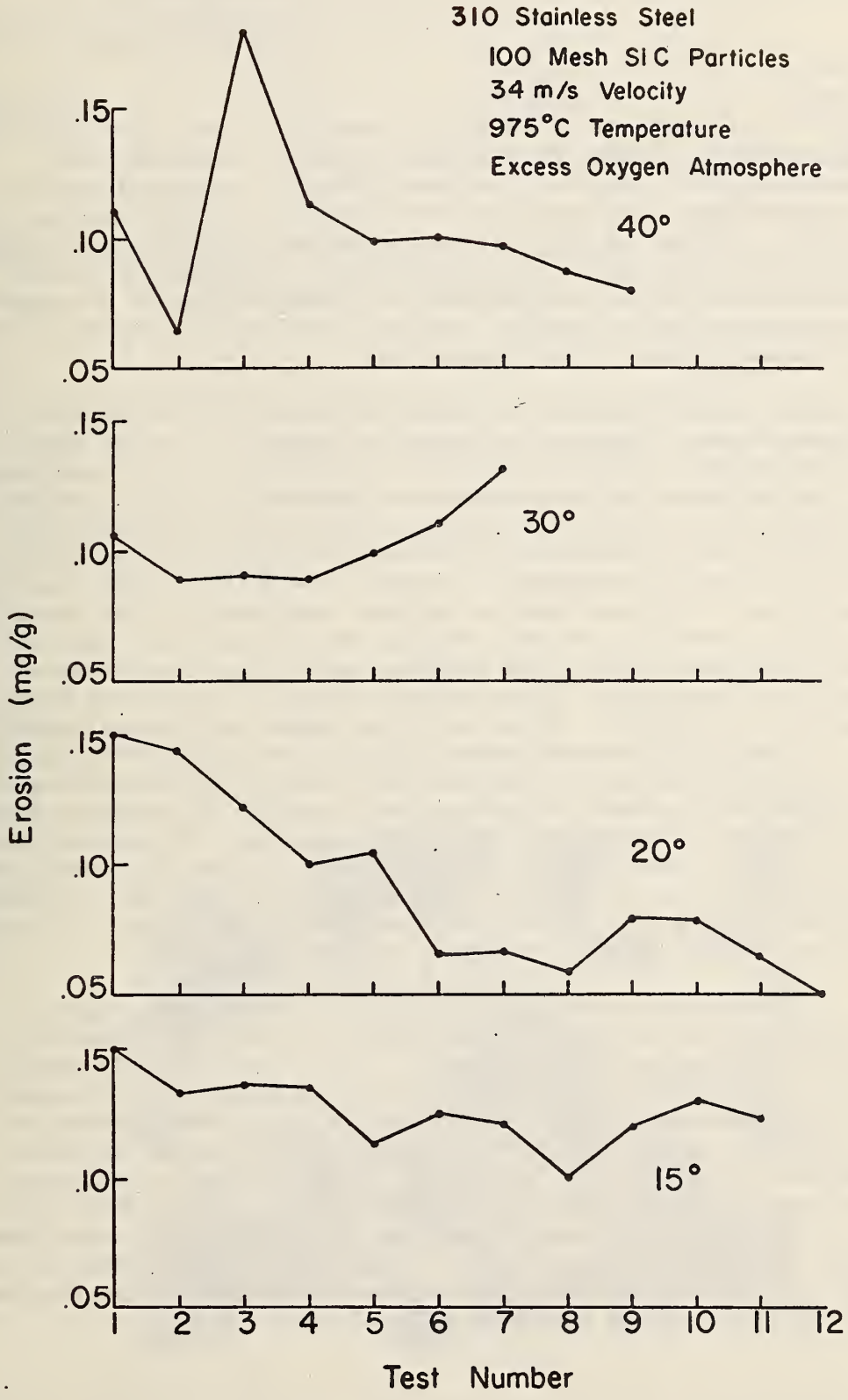

Fig. 4. Trend of erosion rate with test number at 975°C.

2. Ceramic Deformation, Fracture, and Erosion (E. R. Fuller, S. M. Wiederhorn, J. M. Bukowski, C. R. Robbins, and D. E. Roberts, 313.05)

Progress: The majority of the effort in the past quarter has been in the design and construction of the three pressure vessel systems, described in the last quarterly progress report. Additional experiments, however, have been performed which examine: the mechanical behavior of a calcined kaolin, calcium aluminate castable after exposure to environments of CO_2 and steam; the erosion of a phosphate bonded tabular alumina castable; the microstructural morphology of various hydrated calcium aluminate phases; and the dehydration behavior of the calcium aluminate phase, $4CaO.3Al_2O_3.3H_2O$.

Three pressure vessel systems are being developed: to extend the temperature-pressure regime of our previous studies; to allow the introduction of additional environmental components of coal gasification systems; and to permit in situ mechanical property testing. Two of these systems will be used for exposure testing with subsequent mechanical property characterization of exposed specimens and the other system will be used for mechanical property testing under coal gasification conditions. The basic design has been completed for the system in which in situ mechanical property testing can be conducted. All major components have been ordered and construction of the outer pressure shell is nearly completed. Welds in this vessel are presently being radiographically inspected, after which the vessel will be hydrostatically tested. A commercial pressure vessel unit for the exposure testing has arrived and been installed. This unit with its two separate pressure vessel systems will extend the temperature range of the exposure studies to 960¼C (1760¼F) and will allow accurate measurement of gaseous pressure. "Check out" of this unit is still in progress. A steam injection system is being installed on the other system for exposure testing. If operation proves to be satisfactory, a similar steam injection system will be used on the apparatus for in situ mechanical property testing.

A laboratory refractory composition has been prepared from calcined kaolin aggregate and calcium-aluminate cement to produce a castable refractory of approximately 56% alumina, 37% silica, and 4.5% lime. Specimens, prepared from this mixture and fired according to standard practice, have been exposed to environments of CO_2 and CO_2/steam at 610°C (1130°F) and 1,000 psig total pressure. The results of these experiments are tabulated in Table 2.1. X-ray diffraction analysis shows an enhanced crystallization of anorthite ($CaO.Al_2O_3.2SiO_2$) after exposure to the CO_2/steam environment. An example of the cement phase morphology, developed by exposure to this environment, is shown in Fig. 2.1. The strengthened structure appears to be related to the interwoven platelet structure of the anorthite crystallites.

Table 2.1 Properties of a calcined kaolin, calcium-aluminate castable after exposure to environments of CO_2 and steam at 610°C (1130°F) and 1,000 psig total pressure.

Environment	Exposure time	Flexural strength	Mineral phases
As fired, no exposure		1,300 ± 350 psi	cristobalite, mullite, α-alumina, $CaO.2Al_2O_3$, $CaO.Al_2O_3$, anorthite.
CO_2	65 hrs	1,200 ± 220 psi	cristobalite, mullite, α-alumina, $CaO.2Al_2O_3$ $CaO.Al_2O_3$, anorthite.
50% CO_2 and 50% H_2O	20 hrs	2,170 ± 380 psi	cristobalite, mullite α-alumina, anorthite, $CaCO_3$(tr), tridymite(tr).
	165 hrs	2,180 ± 440 psi	

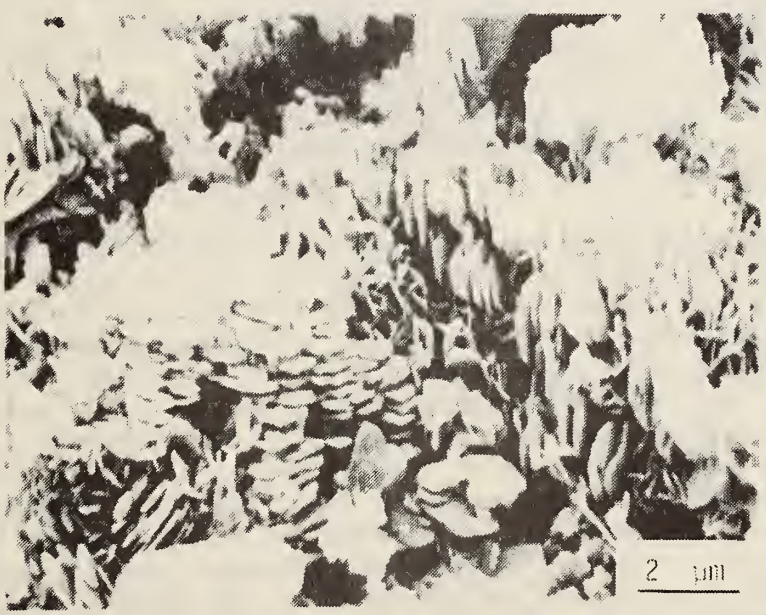

Fig. 2.1. Microstructure of the cementing phase of a calcined kaolin, calcium-aluminate castable after exposure to an environment of 500 psig CO_2 and 500 psig H_2O at 610°C (1130°F).

Erosion data on a phosphate bonded refractory have been collected at room temperature and at 1000°C. The behavior of this refractory at both temperatures is very similar to that observed for the high purity aluminum oxide refractory. Erosion occurs primarily by wear of the cement phase of the refractory so that surface channels develop as the wear process proceeds. As in the case of the high purity alumina refractory, the wear rate can be expressed as a power function of the particle velocity, the wear rate increasing as (particle velocity)$^{2.3}$. The exponent of approximately 2.3 was slightly less than an exponent of 2.8 determined for the high purity aluminum oxide castable. At 1000°C, the erosion rate was about a factor of three less than that measured at 25°C, agreeing with earlier data on the high alumina castable. A comparison of the two types of refractories indicates a somewhat lower rate of erosion for the phosphate bonded refractory, the phosphate bonded refractory being approximately three times as resistant to erosion. This conclusion, however, must be tempered by the fact that erosion studies on the high alumina refractory were conducted on compositions that had been made with relatively large amounts of water. Since the erosion resistance of the refractory depends on the amount of water used in its formation, it may be possible to increase the erosion resistance of the high alumina refractory by decreasing the amount of water used inthe original mix for this refractory.

The microstructural morphology of various hydrated calcium-aluminate phases have been examined by Professor C. H. Kim, a visiting scientist at NBS, using scanning electron microscopy. His observations shows that when a high alumina, calcium-aluminate castable refractory has been treated hydrothermally to form the hydrate $4CaO.3Al_2O_3.6H_2O$, the binding matrix microstructure is loosely connected (see Fig. 2.2) and consequently is probably a major contributing factor in the loss of structural integrity observed in this refractory. In contrast, before this hydrate is formed the integrity of the cementing microstructure is maintained by an interwoven platelet structure of either $3CaO.Al_2O_3.6H_2O$ or boehmite (AlO.OH) (See Fig. 2.3).

Since coal gasification systems operate at temperatures higher than those used in our previous hydrothermal studies, the integrity of refractory liners might not depend as much on the formation of $4CaO.3Al_2O_3.3H_2O$ as on the dissociation of this compound. Although a number of laboratories have reported the dehydration products as $12CaO.7Al_2O_3$ and $CaO.Al_2O_3$ - both in air and under hydrothermal conditions - little attention has been given to the compound $4CaO.3Al_2O_3$, a cubic compound first observed in 1943 and later confirmed by single crystal structure analysis. In anticipation of exposure studies to 960°C (1760°F), a preliminary examination of the dehydration of $4CaO.3Al_2O_3.3H_2O$ in air was initiated. The formation of $4CaO.3Al_2O_3$ has been observed both in calcium-aluminate cement powders and in bar specimens of a high alumina, calcium-aluminate castable after heat treatment at 650°C in air. Subsequent attempts to rehydrate this cubic compound under ambient conditions in 100% relative humidity resulted in the formation of predominantly $CaCO_3$ and gibbsite [Al.()H)$_3$].

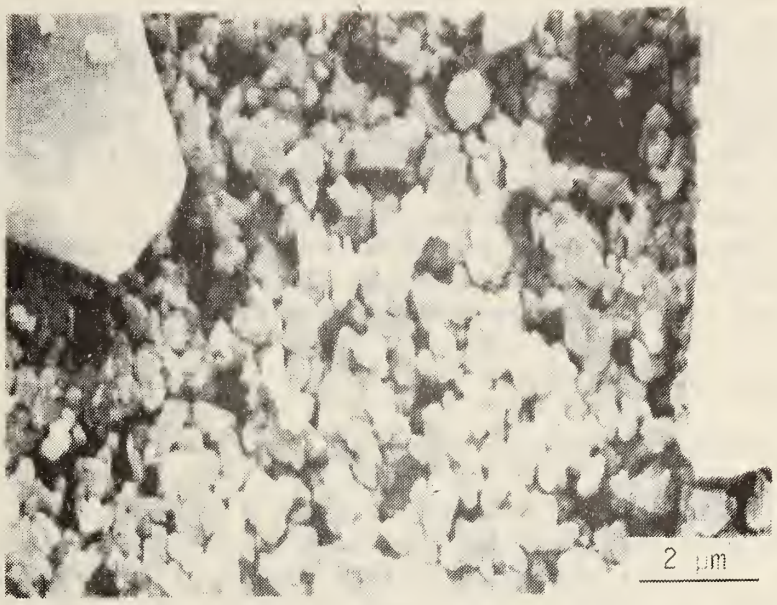

Fig. 2.2. Microstructure of a high-alumina, calcium-aluminate castable after exposure to steam at 375°C and approximately 3,200 psi pressure. The after-exposure flexural strength is 430 ± 90 psi.

Fig. 2.3. Microstructure of a high-alumina, calcium-aluminate castable after exposure to steam at 210°C and 276 psi pressure. The after-exposure flexural strength is 2,230 ± 50 psi.

Plans: Construction of the outer pressure shell for the in situ mechanical properties testing apparatus will be completed and this vessel will be proof-tested and installed. Design of the internal components of this apparatus will be completed and their construction begun. The hydrothermal research unit will be "checked-out" on both high and low alumina calcium-aluminate castables in a steam environment, thus extending our previous hydrothermal results to 910°C (1670°F). Exposure test in CO_2 and steam environment will then be continued. Erosion measurements will be conducted on the phosphate bonded refractory to complete the characterization of its wear behavior as a function of temperature. Work will then begin on a calcined kaolin refractory.

3. Chemical Degradation

a. Reactions and Transformations (F. Mauer and C. R. Robbins, 313.06)

Progress: Design of the pressure vessel for x-ray diffraction measurements has been completed and submitted to the NBS Instrument Shops Division. Material for construction of the pressure vessel has been ordered and construction will begin shortly. The internal heater and specimen mount are to be constructed in the laboratory. A mock-up of the heater has been built and tested. A power input of 150 watts is required to reach a temperature 700 °C above ambient. With the walls of the vessel operating at 300 °C (to prevent condensation) this same power input is expected to heat the specimen to 1000 °C. The boron carbide disks for the x-ray windows have been received. They will have to be ground and polished in the instrument shop to provide a finished surface for the gaskets.

Samples of α-quartz, cristobalite, C_3A, CA, CA_2, AH(Boehmite), α-Al_2O_3, CA_6, $C_{12}A_7$, C_3AH_6, and CAS_2^* have been obtained for use in preparing standard x-ray patterns so that these phases can be recognized. Patterns have been prepared with a conventional x-ray diffractometer using copper radiation. Patterns for the first six listed above have also been prepared by the energy dispersive powder diffraction method that will be used for in situ studies of samples exposed to simulated coal gasification environments. Data from the conventional x-ray patterns are now being transformed so that the corresponding features of the energy dispersive x-ray diffraction patterns (EDXD) can be identified and labled. The labled EDXD patterns will serve as working standards.

Plans: The pressure vessel and ancillary equipment for introducing atmospheres and measuring temperature and pressure will be assembled and checked out during the next quarter. In situ x-ray diffraction measurements are expected to begin by January 1, 1977, according to our original schedule.

*The following abbreviations are used:
C = CaO
A = Al_2O_3
S = SiO_2
H = H_2O

b. Slag Characterization (W.S. Brower, J.L. Waring, 313.03 and D.H. Blackburn, 313.02)

Progress: Analyses of several Montana Rosebud coal ash samples have been obtained from various sources. The initial synthetic slag composition chosen was based on the high calcium content analyses, which are representative of the initial Bigas feel stock. The normalized composition is as follows:

SiO_2	42.10 wt%
Al_2O_3	19.50
Fe_2O_3	7.11
CaO	24.48
Na_2O	0.21
K_2O	0.10
MgO	5.50
TiO_2	0.90

This composition has been prepared for the initial ambient pressure viscosity determinations. Delivery of the gear motor for rotation of the slag container has not been made at this date. As this constitutes the main part of the apparatus, pre-calibration of the bob and cup assembly have not been started.

Plans: The viscosity of the selected slag composition will be determined at ambient pressure as a function of temperature. Calibration of the viscosity apparatus will be completed when the portions of the system that have been ordered arrive.

c. Vaporization and Chemical Transport (J. Hastie and D. Bonnell, 313.01)

Progress: During this reporting period a platinum tube was acquired for fabrication of several high temperature/high pressure reactors. The first of several planned reactor-types has been constructed. This reactor utilizes a well established free jet expansion and skimmer arrangement for conversion of the high temperature/high pressure gas to a molecular beam suitable for mass spectrometric analysis.

Plans: The free jet expansion reactor will be tested and calibrated using an inert gas medium followed by a reactive gas mixture containing NaCl. The calibration procedure will involve monitoring the mass spectral ion intensities for the NaCl and $(NaCl)_2$ species as a function of temperature and total pressure. Comparison of these data with those derived from the JANAF Thermochemical Tables will determine the reliability of the sampling technique for future studies of coal gas mixtures where the literature thermochemical data are incomplete.

4. Failure Avoidance Program (J. H. Smith, 312.01)

Progress: To date approximately 350 items have been received concerning pilot plant operating discrepancies, component failures, quarterly reports from pilot plants, etc. These items have been reviewed and after eliminating duplicates and extraneous items a total of 300 pertinent reports have been abstracted, classified and typed into the CCA Model 204 computerized Data Base Management System. Information has been received from the following pilot plants and PDUS: Battelle, Carbonate, COED, CO_2, CPC, HYGAS, LERC, Lignite, MERC, SRC (Ft. Lewis), SRC (Wilsonville), Synthane and Westinghouse.

Detailed computer programs have been written for the CCA Model 204 computer program which will be used to conduct failure mode analyses to identify critical operating problem areas. Failure reports in the computer can now be sorted by process, material, failure category, component category, any combination of the preceding or all of the preceding. The program will produce an output in the form of a table (Table 1) or as abstracts (Table 2). The program will also make the task of summarizing failure incidences much easier (Table 3).

Two regular meetings of the ERDA - Performance Assurance System Steering Committee were participated in as a regular committee member to make this group aware of the present Failure Avoidance Program. A paper on the Failure Avoidance Program was presented at the first annual ERDA-EPRI-AGA Conference on Materials for Coal Conversion and Utilization held in Germantown, Maryland September 30 - October 1, 1976. Information for the ERDA Newsletter was furnished to Battelle resulting in three failure experiences being reported in the August newsletter. In addition, a series of seven failure reports has been submitted to Battelle for inclusion in future issues of the newsletter. We will be sending Battelle a weekly updating on new material received on failure problems. The Data Center has received many requests for further information based on articles in the April, 1976 ERDA Newsletter. These have come from manufacturers, universities, failure analysis laboratories and consulting engineers.

Plans: The information gathering phase of this task will continue as more information is received on a continuing basis from the pilot plants. In addition, detailed follow-up of certain information already received will be initiated. Additional visits to operating pilot plants will be made to collect additional information.

The information evaluation and processing phase of this program will continue and be enlarged. The operation of the automated data storage system will be enlarged and refined for easier and more efficient use. The information presently in the data base will be used to conduct failure mode analyses to identify critical operating problem areas.

The information dissemination phase of this program will continue and will be developed to include more direct contact with users. At present, several inquiries a month are answered from plant operations and design personnel. Plans have also been initiated to include summary results of this program in the bimonthly ERDA-Materials and Components Newsletter.

Additional information dissemination will take place through the Fossil Energy - Performances Assurance Systems that is currently under development. Close liaison with this program is being maintained.

Table 1

```
I3 6
I3 6
??SEARCH.CRITERIA
FAILURE CATEGORY = EROSION AND COMPONENT CATEGORY = PIPING OR PUMPS
??KEY
PROCESS
```

I.N.	PROCESS	MATERIAL	FAILURE	COMPONENT
25	CO2	304 S.S. 316 S.S. CARBON STEEL S.S. STEEL	CORROSION	PIPING PUMPS VALVES
290	CO2	UNKNOWN	EROSION EQUIP.MALF. OVERHEATING	PIPING
12	HYGAS	CARBON STEEL A105 A53 A243	EROSION	PIPING
42	HYGAS	STELLITE INCOLOY 800 CAST STEEL STEEL 304 S.S. 446 S.S. S.S.	CORROSION EROSION	PUMPS VALVES PIPING
51	HYGAS	STELLITE	EROSION	PIPING
210	HYGAS	INCOLOY 800	EROSION	PIPING BELLOWS
206	HYGAS	CARBON STEEL STEEL	CORROSION EROSION	PIPING COOLING BU
301	LERC		EROSION DESIGN	PIPING VALVES
234	LIGNITE	UNKNOWN	SCC CORROSION EROSION	PIPING PREHEATER HEAT EXCHA THERMOWELL
31	SRC	SEVERAL	EROSION DESIGN	PUMPS

Table 2

```
IS 8
IS 8
??SEARCH.CRITERIA
FAILURE CATEGORY = EROSION AND COMPONENT CATEGORY = PIPING OR PUMPS
??KEY
PROCESS

I.N.  PROCESS      MATERIAL        FAILURE                    COMPONENT
210   HYGAS        INCOLOY 800     EROSION                    PIPING

 TELECON,5/5/76,FROM S.GREENBERG,ANL,TO B.ORCHARD,IGT.
 EXPANSION JOINT-GASIFIER TRANSFER LINE.
                              ABSTRACT
 COAL PRODUCT-METAL REACTION PRODUCTS ARE FOUND GENERALLY ON BOTH SIDES OF
 THE BELLOWS AND IN ALL AREAS.IT SEEMS UNLIKELY THAT CORROSION IS THE MAIN
 CAUSE OF BELLOWS PERFORATIONS.
   CURRENT VIEWS ARE THAT THE PITS ARE DUE TO EROSION,AT LEAST IN THE
 CASE OF INTERNAL SURFACE PITS.PITTING WAS PRECEDED BY LOCALIZED FAILURE OF
 THE LINER TUBE ALLOWING PARTICAL IMPINGEMENT ON THE INTERIOR BELLOWS SURFACE.
AFTER PERFORATION OF THE BELLOWS THE STRUCTURE OF THE TRANSFER LINE ASSEMBLY
 ALLOWED PARTICLE IMPINGEMENT ON THE EXTERIOR SURFACE OF THE BELLOWS.
   IT IS IMPORTANT TO EXAMINE THE REMAINDER OF THE BELLOWS AND ESPECIALLY
 THE LINER TUBE.
 SEE I.N. 186,194,236,274,285,286 FOR FURTHER INFORMATION.
◆

I.N.  PROCESS      MATERIAL        FAILURE                    COMPONENT
301   LERC                         EROSION                    PIPING

 REPORT,8/10/76,FROM A.WEST,SANDIA LABS,TO H.FRANKEL,ERDA.
 REVIEW OF MATERIALS PROBLEMS AT LERC IN-SITU GASIFICATION FACILITY
                              ABSTRACT
 1.PIPE ELBOW EROSION: ELBOWS SHOWED SIGNS OF IMPACT BY LARGE SIZED PARTICULATES
   THAT EXIT THE PRODUCTION WELL NEAR THE END OF A BURN.THIS CAN BE DRASTICALLY
   REDUCED BY USE OF APPROPRIATE BAFFLING OR USE OF CYCLONES TO PREVENT
   PARTICULATES FROM LEAVING THE WELL.
 2.CHILL RING EROSION: RESULTS FROM RING PROTRUDING INTO THE FLOW PATH OF
   EXITING GAS/W PARTICULATES.CHILL RINGS ARE USED FOR ALIGNMENT DURING MANUAL
   FIELD WELDING OF PIPES.THE USE OF AUTOMATED WELDING PROCEDURES WITH
   APPROPRIATE ALIGNMENT FIXTURES SHOULD ELIMINATE THE NEED FOR CHILL RINGS.
 3.VALVES: THE PRIMARY PROBLEM AT LERC HAS BEEN THE GUMMING UP OR JAMMING
   OF BOTH BALL AND GATE VALVES DUE TO HARDENING OF COAL TAR IN THE VALVE SEATS.
 4.STACK COLLAPSE: THE STACK FOR BURNING OFF GASES COLLAPSED DUE TO POOR DESIGN.
◆
```

Table 3

FREQUENCY OF FAILURE MODE

Cause of Incident	No. of Items	CO_2	Hygas	SRC	Synthane	Others
Undetermined	20	5	7	3	5	
Sulfidation	18	10	8			
Erosion	17	1	4	6	5	1
Corrosion	78					
Pitting	4	2	2			
Dusting	3	3				
Carb.	8	6	2			
General	63	28	18	4	11	2
Design Defect	11					
General	7	3		3		1
Thermal Stresses	4		2	2		
SCC - CL	15	5	5		2	3
Fabrication	7	2				
Welding	5	1	2		1	1
Quality Control	8	4	1		1	2